

Orbital and spin chains in ZnV_2O_4

S.-H. Lee¹, D. Louca², H. Ueda³, S. Park¹, T.J. Sato⁴, M. Isobe³, Y.

Ueda³, S. Rosenkranz⁵, P. Zschack⁶, J. Íñiguez¹, Y. Qiu¹, and R. Osborn⁵

¹*NIST Center for Neutron Research, National Institute of Standards and Technology, Gaithersburg, MD 20899*

²*Department of Physics, University of Virginia, Charlottesville, VA 22904*

³*Institute for Solid State Physics, University of Tokyo, Kashiwa, Chiba 277-8581, Japan*

⁴*National Institute for Materials Science, Tsukuba, Ibaraki 305-0047, Japan*

⁵*Material Science Division, Argonne National Laboratory, Argonne, IL 60439*

⁶*Frederick-Seitz Materials Research Lab, University of Illinois at Urbana-Champaign, IL 61801*

(Dated: January 27, 2020)

Using single crystal synchrotron X-ray diffraction and powder inelastic neutron scattering, we show that ZnV_2O_4 is a system of spin chains that are three dimensionally tangled in the cubic phase above 50 K due to randomly occupied t_{2g} orbitals of V^{3+} ($3d^2$) ions. Below 50 K in the tetragonal phase, the chains become straight due to antiferro-orbital ordering. This is evidenced by the characteristic wave vector dependence of the inelastic neutron scattering data that changes from symmetric to asymmetric at the cubic-to-tetragonal transition.

Cubic spinels, AB_2O_4 , with magnetic B ions have attracted considerable attention recently in light of geometrical frustration intrinsic to the B-site sublattice of corner-sharing tetrahedra[1]. The long sought zero energy mode of spin fluctuations in the B sublattice[2, 3] was found in ZnCr_2O_4 [4]. Also in ZnCr_2O_4 , a spin-Peierls-like transition to relieve frustration was found upon cooling where a tetragonal distortion and a magnetic long range order occur simultaneously[5]. When the B site is occupied by vanadium ions with orbital degeneracy, complex electronic and magnetic properties emerge. LiV_2O_4 , for instance, with monovalent Li ions at the tetrahedral A site and mixed valent $\text{V}^{3.5+}$ ions exhibits heavy fermion (HF) behavior at low temperatures with the largest Sommerfeld constant among d -electron systems, $\gamma \approx 0.42$ J/mol K²[6]. AV_2O_4 with divalent ions such as Zn [7], Mg [8], Cd [9], at the A site and trivalent V^{3+} ($3d^2$) ions is a Mott insulator [10] that undergoes two separate phase transitions at low temperatures, in contrast to other insulating spinels without orbital degeneracy such as ZnCr_2O_4 . In this Letter, we show that the orbital degree of freedom plays the central role in the physics of vanadates.

Many theoretical efforts have been made to understand the unusual low temperature behaviors of metallic and insulating vanadates. The macroscopic ground state degeneracy induced by the geometrical frustration intrinsic to the magnetic lattice was attributed to explain the enhancement of the specific heat at low temperatures in LiV_2O_4 [11]. It was also used to explain why the Néel temperature, T_N , is considerably lower than the Curie-Weiss temperature, Θ_{CW} , in the insulating vanadates. Spin-lattice coupling mechanisms have been proposed to explain the phase transitions of ZnV_2O_4 [12, 13], but fail to explain why the spin and lattice order at different temperatures in the insulating vanadates unlike in ZnCr_2O_4 . Orbital degeneracy of the vanadium ions was recently considered as well. Fulde *et al.* proposed

[14] that due to frustrated charge order or orbital order in LiV_2O_4 ($3d^{1.5}$), one-dimensional chains form, that contribute to the enhancement of the linear term in the specific heat. For insulating AV_2O_4 ($A = \text{Zn, Mg, Cd}$) ($3d^2$), Tsunetsugu and Motome proposed [15] that in the tetragonal ($c < a = b$) phase, among the triply degenerate t_{2g} orbitals, the d_{xy} orbital is favored and is occupied by one electron at every V site. The second electron is in an antiferro-orbital state that can be described by stacking the ab -planes along the c -axis with alternating d_{yz} and d_{zx} orbitals. This effectively forms straight spin chains on the ab -planes. Using a crystal symmetry argument, a ferro-orbital model for the orbital state of the second electron was also proposed [16, 17]. To test the validity of these theoretical models, detailed studies of magnetic correlations and crystal structure in the vanadates are necessary to elucidate the interplay between spin, orbital, and lattice degrees of freedom.

We have studied the insulating ZnV_2O_4 that exhibits a tetragonal transition at 50 K and a magnetic long range order at 40 K with an ordered moment $\langle M \rangle = g \langle S \rangle = 0.61(3) \mu_B/V$, in spite of strong magnetic interactions evidenced by $|\Theta_{CW}| = JzS(S+1)/3k_B = 998(5)$ K [7, 18, 19]. Earlier crystal structure studies on powder samples [18, 19] reported that the cubic and tetragonal phases have high symmetries, $Fd\bar{3}m$ ($a = 8.39941(5)$ Å) and $I4_1/amd$ ($a_t = 5.94807(5)$ Å $\approx a/\sqrt{2}$ and $c_t = 8.37532(1)$ Å), respectively. However, our single crystal synchrotron X-ray diffraction measurements have shown the existence of additional weak nuclear reflections both in the cubic and tetragonal phases that are *forbidden* for the commonly used symmetries. Instead the symmetry of the cubic structure is best described by $F\bar{4}3m$. The symmetry of the tetragonal phase can be either $I\bar{4}m2$ or $I\bar{4}$ that is compatible with the ferro- or the antiferro-orbital state models. When the tetragonal distortion occurs, the wave vector (Q) dependence of our inelastic magnetic neutron scattering from the powder

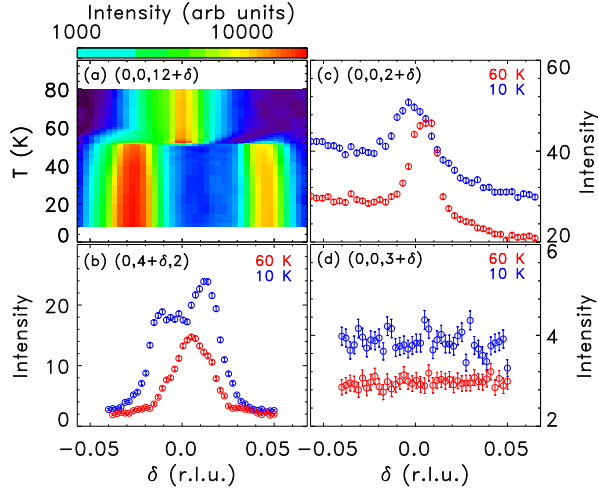


FIG. 1: Synchrotron X-ray data obtained from a single crystal of ZnV_2O_4 . (a) Color contour map of the (0,0,12) nuclear Bragg peak intensity as a function of temperature and wave vector. Intensities at 10 K and 60 K for (b) the (0,4,2), (c) (0,0,2), and (d) (0,0,3) reflections.

sample changes lineshape from a symmetric centered at $Q_c^{\text{cubic}} = 1.35(4) \text{ \AA}^{-1}$ to an asymmetric one peaked at $Q_c^{\text{tetra}} = 1.10(2) \text{ \AA}^{-1}$. Quantitative analysis shows that ZnV_2O_4 is a system of three-dimensionally tangled spin chains in the cubic phase. In the other hand, in the tetragonal phase ZnV_2O_4 becomes an excellent model system for one-dimensional spin chains. This favors the antiferro-orbital model that yields straight chains in the *ab*-planes with *weak* interchain interactions. We argue that our findings provide a unified picture of the physics of vanadates, both insulating and metallic.

A single crystal with dimensions of 10^{-3} mm^3 (0.06 mg) and a 30 g polycrystalline sample of ZnV_2O_4 were used for the synchrotron X-ray and neutron scattering experiments, respectively. The X-ray measurements were carried out at the 33BM-C beamline at the Advanced Photon Source of Argonne National Laboratory. The inelastic neutron scattering measurements were performed using the time-of-flight spectrometer LRMECS at the Intense Pulsed Neutron Source with an incident energy, $E_i = 30 \text{ meV}$.

Fig. 1 summarizes the synchrotron X-ray data obtained from the ZnV_2O_4 single crystal. For simplicity, we used the cubic notation with lattice constant *a* for the tetragonal as well as the cubic phases. Fig. 1 (a) shows the (0,0,12) nuclear Bragg peak that splits into two below 50 K due to the tetragonal distortion. But as shown in Figs. 1 (b) and (c), several newly found weak nuclear reflections at $(0, 2k, l)$ with $l = 2n$ (*n* is an integer) and at $(0, 0, l)$ with $l = 2n$, *forbidden* for $Fd\bar{3}m$ as well as for $I4_1/amd$ symmetries unless $2k + l = 4n$ [20], exist above and below 50 K. Intensities of these new nuclear Bragg peaks are three orders of magnitude weaker

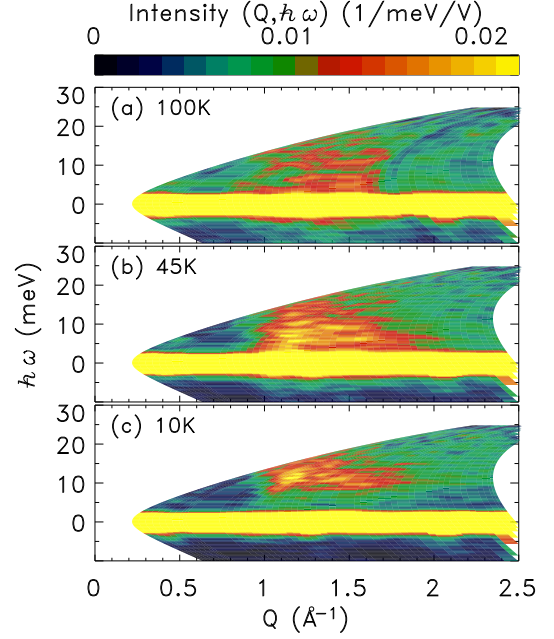


FIG. 2: Neutron scattering intensity as a function of energy ($\hbar\omega$) and wave vector (Q) transfer obtained from a powder sample of ZnV_2O_4 at three different phases. (a) At 100 K, in the cubic and cooperative paramagnetic phase. (b) At 45 K, in the tetragonal phase without magnetic long range order. (c) At 10 K, in the tetragonal and Néel phase.

than a typical main peak. The $(0, 0, l)$ reflections with odd *l* were absent (see Fig. 1 (d)). These data unequivocally indicate that the symmetry of the cubic structure of ZnV_2O_4 is $F43m$ while that of the tetragonal phase is either $I4m2$ or $I4$. These two tetragonal symmetries have the same reflection conditions consistent with our data. Their difference is that $I4m2$ has mirror planes in the $\{110\}$ planes whereas $I4$ does not [20].

Fig. 2 is an overview of the inelastic magnetic neutron scattering data in the form of color images of intensity, $I(Q, \hbar\omega)$, as a function of Q and energy transfer, $\hbar\omega$, in three different phases. In the cubic phase I ($T > 50 \text{ K}$), strong low energy magnetic excitations are present in the form of a broad peak centered at $Q_c^{\text{cubic}} = 1.35(4) \text{ \AA}^{-1}$ shown in Fig. 2(a). In phase II ($40 \text{ K} < T < 50 \text{ K}$) with the tetragonal distortion but no magnetic long-range order, a similar broad peak is present at low energies. However, the broad peak is strikingly asymmetric in Q and shifts to a lower characteristic wavevector, $Q_c^{\text{tetra}} = 1.10(2) \text{ \AA}^{-1}$ (Fig. 2 (b)). In the tetragonal Néel phase III ($T < 40 \text{ K}$), the asymmetry of the broad feature in Q remains but most spectral weight in the inelastic scattering cross section shifts in energy and is concentrated around 11 meV (Fig. 2 (c)). The change from symmetric to asymmetric Q -dependence of the spin excitations between 100 and 45 K indicates that there is a crossover in the nature of the magnetic correlations from three dimensions to a lower dimension [21] between

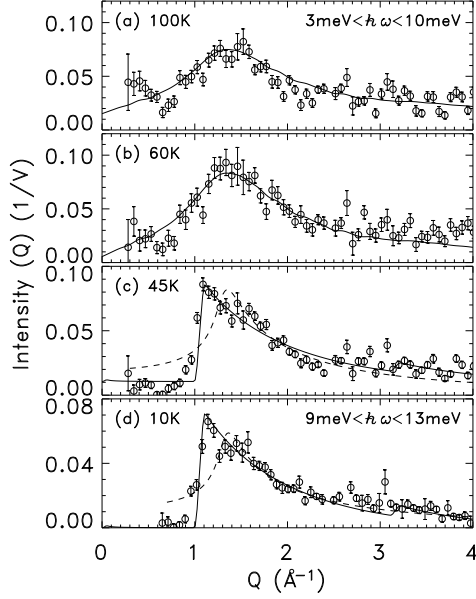


FIG. 3: Q -dependence of inelastic neutron scattering intensity obtained by integrating the data shown in Fig. 1 over the range of energy that includes most of the excited spectral weight: (a) at 100 K, (b) 60 K, (c) 45 K, and (d) 10 K. The energy integration range is $3 \text{ meV} < \hbar\omega < 10 \text{ meV}$ for (a), (b) and (c) and $9 \text{ meV} < \hbar\omega < 13 \text{ meV}$ for (d). Lines are fits to the models explained in the text.

phases I and II.

The energy integrated inelastic neutron scattering intensity as a function of Q is shown at several temperatures in Fig. 3. In phase I of the 60 and 100 K data, the broad peak centered around $1.35(4) \text{ \AA}^{-1}$ can be attributed to cooperative paramagnetic spin fluctuations induced by geometrical frustration intrinsic to the magnetic lattice. However, the peak position ($Q_c^{\text{cubic}} = 1.35(4) \text{ \AA}^{-1}$) is different from $Q_c = 1.5 \text{ \AA}^{-1}$ expected when antiferromagnetic hexagonal spin loops are the fundamental spin degrees of freedom in ZnV_2O_4 as in ZnCr_2O_4 [4, 5, 13]. Instead, an orbital model similar to the one proposed in Ref. [14] was considered. Since in the cubic phase the three t_{2g} orbitals, d_{xy} , d_{yz} , and d_{zx} , are equivalent, we assume that at each V site the their occupancy fluctuates with time with an equal probability of $1/3$. At an instant time, two out of the three orbitals are randomly occupied at all V^{3+} sites. We considered a model with $12 \times 12 \times 12$ cubic unit cell with such randomly occupied t_{2g} orbitals. Fig. 4 (a) shows a schematic representation of one such unit cell. We subsequently consider all possible magnetic interactions due to direct overlap of the orbitals to obtain the effective fluctuating spin objects. Shown as sky blue rods in Fig. 4 (a), the resulting fluctuating spin objects form three-dimensionally tangled antiferromagnetic spin chains. The solid lines in Fig. 3 (a) and (b) are the powder-averaged result-

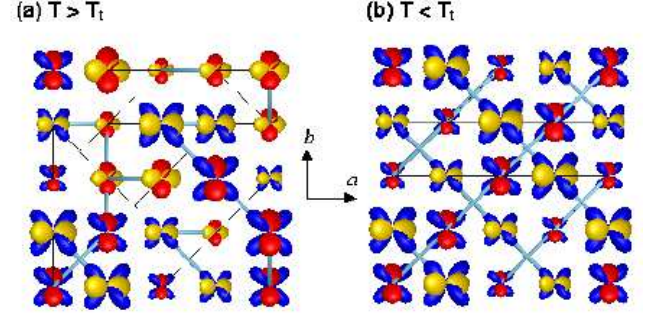


FIG. 4: (a)-(b) Illustrations of the orbital states of ZnV_2O_4 in one cubic unit cell. Balloons represent the t_{2g} orbitals of the $\text{V}^{3+}(3d^2)$ ions: d_{xy} (blue), d_{yz} (red), and d_{zx} (yellow) orbitals located at the vanadium site. The four different sizes of the balloons represent four different ab -planes with different z -coordinates. (a) The cubic phase above 50 K. The three orbitals are randomly distributed. The blue rods connect possible dynamic magnetic interactions at a snap shot due to direct overlap of the neighboring orbitals. (b) Antiferro-orbital model for the tetragonal phase.

ing structure factor squared from this model that reproduces the data well including the characteristic wave vector Q_c^{cubic} .

In the tetragonal phases II and III, spin fluctuations change dramatically, with a sharp increase at low Q and a long tail at high Q . In Fig. 3(c) and 3(d), the dashed lines are fits to a two-dimensional Lorentzian [22] whereas the solid lines are fits to the dynamic structure factor for a one dimensional (1D) spin chain given by [23],

$$S(\vec{Q}, \omega) \propto |F(Q)|^2 \frac{1 - \cos(\vec{Q} \cdot \vec{d})}{\hbar\omega_{\vec{Q}}} \delta(\omega - \omega_{\vec{Q}}), \quad (1)$$

after powder averaging. Here $F(Q)$ is the magnetic form factor for the V^{3+} and the spin wave dispersion relation is $\hbar\omega_{\vec{Q}} = \sqrt{\Delta^2 + v^2 \sin^2(\vec{Q} \cdot \vec{d})}$ where Δ is a spin gap and v is the spin wave velocity. The optimal intrachain spacing, d , obtained from the fitting is consistent with the distance between nearest neighboring V^{3+} ions: $d = \pi/Q_c^{\text{tetra}} = 2.97 \text{ \AA} = a_t/2$. The excellent agreement between the 1D chain model and data shows that below the tetragonal transition, ZnV_2O_4 is a system of one dimensional antiferromagnetic spin chains. This one-dimensionality of the magnetic interactions can be understood if two orbitals per V ion are occupied in a striated form along the c -axis, as shown in Fig. 4(b). One electron from every V ion resides in the d_{xy} orbital while the occupancy of the second electron can be described by stacking the ab -planes with alternating d_{yz} and d_{zx} orbitals along the c -axis [15]. The direct overlap of neighboring t_{2g} orbitals occurs only between d_{xy} orbitals, yielding orbital chains and thereby one dimensional antiferromagnetic spin chains in the ab -planes. The V^{3+} magnetic moments do not order even in the orbitally ordered

state because of the one-dimensionality of the magnetic interactions until weak interchain interactions, J' , set in. From the mean field (MF)/random phase approximation (RPA) theory for coupled spin chains [24], we estimate J' from the relation between T_N and J' , where $|J'| = k_B T_N / \{1.28 \sqrt{\ln(J/k_B T_N)}\}$ and obtain $|J'| \sim 2$ meV. A ferro-orbital ordering where the second electron of every V^{3+} ion resides on the same orbital that is a linear combination of d_{xy} and d_{yz} , has also been proposed [17]. However, it produces stronger interchain interactions by at least $|J'| \sim 0.25J$ [16] and therefore would generate much less asymmetric lineshape of $S(Q)$ than observed.

Until now, ZnV_2O_4 was considered to be a geometrically frustrated magnet similarly to $ZnCr_2O_4$ because the magnetic V^{3+} ions form a lattice of corner-sharing tetrahedra in the crystal structure. However, our results show that due to the orbital degree of freedom ZnV_2O_4 should be considered as a system of spin chains, instead. In the cubic phase, the random occupancy of the t_{2g} orbitals renders a system of three-dimensionally tangled spin chains. In the tetragonal phase ($c < a = b$), on the other hand, antiferro-orbital ordering occurs that yields a system of weakly interacting straight spin chains in the ab planes. This picture can also be used to explain the phase transitions observed in other insulating vanadates, AV_2O_4 ($A = Mg$ and Cd). The tetragonal transition occurs at $T_t = 65$ K and 97 K whereas the Néel ordering occurs at $T_N = 42$ K and 35 K for Mg and Cd , respectively. T_t is determined by the balance among thermal energy, the energy gain from orbital ordering and the energy cost for the lattice distortion. When the A site is occupied by an ion with much larger ionic size, such as Cd^{2+} than Zn^{2+} and Mg^{2+} , the lattice becomes softer and the tetragonal distortion occurs at a higher temperature. T_N , on the other hand, is determined by the strength of interchain coupling, and therefore it is lower for Cd^{2+} where the interchain coupling is weaker due to the larger distance between V ions.

These results may have significant implications on the physics of metallic LiV_2O_4 as well. In the attempts to understand the heavy fermion behavior in LiV_2O_4 in spite of strong on-site Hund's coupling and with only the d -electrons crossing the Fermi level, several theoretical models have been proposed. These include a Kondo type model where two species of electrons exist at the same site [25], a geometrical frustration model where the macroscopic ground state degeneracy enhances the density of states at low T [11], and a model of spin chains due to frustrated charge or orbital order [14]. Our finding that the cubic phase of ZnV_2O_4 consists of three-dimensionally tangled fluctuating spin chains suggests that the one-dimensionality of the magnetic fluctuations may play an important role in LiV_2O_4 that remains cubic down to 20 mK [26]. It was previously found that LiV_2O_4 exhibits strong antiferromagnetic spin fluctua-

tions when the system enters the heavy fermionic phase at low temperatures [27]. If we consider that the orbital degree of freedom is important in this system as in the cubic phase of ZnV_2O_4 , then the formation of three dimensionally tangled fluctuating orbital chains may also occur in LiV_2O_4 . The metallic character of LiV_2O_4 may produce a spin-density-wave along the orbital chains that is responsible for the strong antiferromagnetic spin fluctuations and the enhancement of the low energy density of states at low temperatures.

We thank D. I. Khomskii, C. Broholm and J. B. Goodenough for valuable discussions. This work was partially supported by the NSF under Agreement No. DMR-9986442 and the DOE under Contracts DE-FG02-01ER45927, W-31-109-ENG-38, DE-FG02-91ER45439, and DE-AC05-00OR22725.

-
- [1] A. P. Ramirez, Handbook on magnetic materials Vol. **13** (ed. Busch, K.J.H.), 423 (Elsevier Science, Amsterdam, 2001).
 - [2] R. Moessner and J. T. Chalker, Phys. Rev. Lett. **80**, 2929 (1998); Phys. Rev. B **58**, 12049 (1998).
 - [3] B. Canals and C. Lacroix, Phys. Rev. Lett. **80**, 2933 (1998).
 - [4] S.-H. Lee *et al.*, Nature **418**, 856 (2002).
 - [5] S.-H. Lee *et al.*, Phys. Rev. Lett. **84**, 3718 (2000).
 - [6] S. Kondo *et al.*, Phys. Rev. Lett. **78**, 3729 (1997); Phys. Rev. B **59**, 2609 (1999).
 - [7] Y. Ueda *et al.*, J. Phys. Soc. Jpn. **66**, 778 (1997).
 - [8] H. Mamiya *et al.*, J. Appl. Phys. **81**, 5289 (1997).
 - [9] N. Nishiguchi and M. Onoda, J. Phys.: Condens. Matter **14**, L551 (2002); M. Onoda and J. Hasegawa, J. Phys.: Condens. Matter **15**, L95 (2003).
 - [10] A. Fujimori *et al.*, Phys. Rev. B **38**, 7889 (1988).
 - [11] V. Eyert *et al.*, Europhys. Lett. **46**, 762 (1999).
 - [12] Y. Yamashita and K. Ueda, Phys. Rev. Lett. **85**, 4960 (2000).
 - [13] O. Tchernyshyov *et al.*, Phys. Rev. Lett. **88**, 067203 (2002); Phys. Rev. B **68**, 144422 (2003).
 - [14] P. Fulde *et al.*, Europhys. Lett. **54**, 779 (2001).
 - [15] H. Tsunetsugu and Y. Motome, Phys. Rev. B **68**, 060405 (2003).
 - [16] D. I. Khomskii, private communication.
 - [17] O. Tchernyshyov, con-mat/0401203 (2004).
 - [18] S. Niziol, Phys. Stat. Sol. **A18**, K11 (1973).
 - [19] M. Reehuis *et al.*, Euro. Phys. J. B **35(3)**, 311 (2003).
 - [20] *International tables for crystallography* Vol. A (ed. Th. Hahn), (Kluwer Academic Publishers, 2002).
 - [21] B. E. Warren, Phys. Rev. **59**, 693 (1941).
 - [22] C. Broholm *et al.*, Phys. Rev. Lett. **65**, 3173 (1990).
 - [23] G. Xu *et al.*, Phys. Rev. B **54**, R6827 (1996); L. P. Regnault and J. P. Renard, Physica B **215**, 71 (1995).
 - [24] H. J. Schulz, Phys. Rev. Lett. **77**, 2790 (1996).
 - [25] V. I. Anisimov *et al.*, Phys. Rev. Lett. **83**, 364 (1999).
 - [26] A. Koda *et al.*, Phys. Rev. B **69**, 012402 (2004).
 - [27] S.-H. Lee *et al.*, Phys. Rev. Lett. **86**, 5554 (2001).